CrystEngComm

Accepted Manuscript

ROYAL SOCIETY OF CHEMISTRY

www.rsc.org/crystengcomm

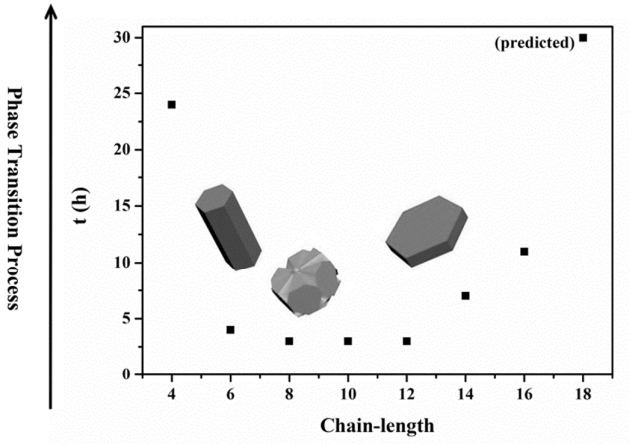

In this work, ligand dynamic effect was utilized to synthesize hexagonal $NaYF_4$ (β-$NaYF_4$) crystals with controllable morphology by a hydrothermal method.

Cite this: DOI: 10.1039/c0xx00000x

www.rsc.org/xxxxxx

ARTICLE TYPE

Ligand Dynamic Effect on Phase and Morphology Control of Hexagonal $NaYF_4$

Suli Wu, Ye Liu, Jie Chang, Shufen Zhang*

Received (in XXX, XXX) Xth XXXXXXXXX 20XX, Accepted Xth XXXXXXXXX 20XX

DOI: 10.1039/b000000x

In this work, ligand dynamic effect was utilized to synthesize hexagonal $NaYF_4$ (β-$NaYF_4$) crystals with controllable morphology by a hydrothermal method. A series of fatty acids were chosen as organic ligands to investigate the ligand dynamic effect on the crystal morphology. Confirmed by scanning electronic microscopy (SEM), transmission electron microscopy (TEM), and X-ray power diffraction (XRD), the dynamic nature of ligands shows strong influences on the crystal morphology, crystal growth and phase transition processes. Also, possible crystal growth processes with different chain length ligands have been proposed.

Introduction

$NaYF_4$ is one of the best luminescent host matrixes for its low lattice phonon energy and transparency in the range of visible and ultraviolet, which could significantly reduce the fluorescence quenching and expand the usability in optical applications.[1] $NaYF_4$ usually crystallizes in cubic (α-) or hexagonal (β-) phase. However, β-$NaYF_4$ is more effective than the particles possessing cubic structure during the upconversion process.[2] The controlled synthesis of β-$NaYF_4$ crystals has become an important issue for their applications in the field of color display[3], bioimaging[4-6], optical detection[7-8], optical devices[9-10] and solar cells[11]. Furthermore, β-$NaYF_4$ crystals are an ideal material for the research of crystal growth due to their unique dissolution-recrystallization growth process.[12-14] In addition, β-$NaYF_4$ crystals have low toxicity and chemical stability, which is propitious to both fundamental and practical research.[15-16]

Over the past decades, morphology control of nano- or microscale inorganic materials has moved into focus for the so-called size- and shape-dependent physical properties of these materials.[17-19] Up to now, many efforts have been made to the preparation of β-$NaYF_4$ crystals with various morphologies by different methods.[20-24] Meanwhile, it is necessary to investigate the influence of different synthesis conditions on crystal growth, so as to reveal the growth mechanism and realize the controlled synthesis of β-$NaYF_4$ crystals. The effect of NaF on both the morphology and phase transition of $NaYF_4$ crystals have been reported by Zhao and co-workers.[25] With the increasing of NaF/Ln ratio, the dimension of $NaYF_4$ crystals becomes larger and the surface gets smoother. It has also been revealed that the phase transition process is accelerated with a higher NaF/Ln ratio. In another report, the effect of NaOH has been studied by Zhang et al.[14] The as-prepared β-$NaYF_4$ crystals exhibit in nanorod, nanotube and nanodisk morphologies by using different amount of NaOH. And decreasing the concentration of NaOH can inhibit the phase transition process. Moreover, ligands play an important role in the shape and size controlled synthesis. Branched $NaYF_4$ has been successfully synthesized with CTAB as ligands.[27] Small and efficient β-$NaYF_4$ nanocrystals in 10 nm scale have been fabricated with oleylamine as ligand at 300 °C by a decomposition method.[28]

Organic ligands in the growth medium of nanocrystals can be selectively adhered to different crystal facets. For the benefit of crystal growth, the ligands need to switch "on" and "off" the growing crystals, so that crystal surfaces are transiently accessible for growth.[29] Surface ligand dynamics has been researched and applied in QDs systems. By using a series of amines as ligands, it has been revealed that ligand dynamic effect on the surface of CdSe nanocrystals is significantly influenced by the ligand chain length.[30] Moreover, the chain-length dependence phenomenon has been proved to originate from the interligand interaction. That's to say, with the increasing of the chain length, the interligand interaction and the boiling/melting point of ligands increase. Thus, when the ligand chain length increases, the ligands are less mobile and the tendency of the ligand leaving the crystal surface will decrease. This theory has also been applied in the research of the oriented attachment of nanoparticles because of the different dynamic nature between short ligands and long ones. Semicircular-shaped bent CdS nanowires have been synthesized from the oriented attachment of CdS nanoparticles by choosing a long chain ligand and a short chain ligand.[31]

However, the studies of ligand dynamic effect are mainly focused on semiconductor quantum dots. Applying ligand dynamic effect to other nano/microcrystals will provide a potentially general way to control morphology of nano- or micro-materials. In this work, we introduce the concept of ligand dynamics into the controlled synthesis of β-$NaYF_4$ crystals by hydrothermal method for the first time. A series of fatty acids with only one anchoring group and a hydrocarbon chain were selected, which favored both the selective coordinating to crystal

surfaces and the growth of $NaYF_4$ crystals. Under given synthesis conditions (F^-/Y^{3+}=4, 200 °C, 7 h), microrods, microprisms with pointed centers, disk-like nano/submicroplates with different aspect ratios were successfully synthesized. To the best of our knowledge, microprisms with star-like centers, microdisks with sunflower-like top/bottom surfaces and microdisks with spire-like centers haven't been reported before. Then, a systematical research of time-dependent experiments was undertaken to study the effect of different ligands on the crystal growth and phase transition processes. It was found that the crystal growth process varies with different chain-length ligands and was clearly classified into three categories. When the ligand chain length was short, the crystal growth experienced a ball-flower-like aggregation stage. In addition, the chain length of ligands significantly influenced the α→β phase transition process, which has not been reported ever before.

Experimental Section

Materials

$Y(NO_3)_3$•$6H_2O$ (99.0%) and chemically pure chemicals of hexanoic acid and decanoic acid were purchased from Sinopharm chemicals reagents Corporation. Analytical grade chemicals of caprylic acid, palmitic acid and NaOH were purchased from Tianjin Bodi Chemical Corporation. Chemically pure chemicals of lauric acid were purchased from Beijing Chemical Factory. Analytical grade chemicals of myristic acid and NaF were purchased from Tianjin Kermel Chemical Reagents Corporation. Analytical grade chemicals of stearic acid and oleic acid were purchased from Tianjin Damao Chemical Reagents. Absolute ethanol was purchased from Tianjin Fuyu Fine Chemical Corporation. All reagents were used directly without further purification and all solutions were prepared using deionized water.

Sample preparation

In a typical synthesis, 1.8 mL 0.5 M $Y(NO_3)_3$ aqueous solution, 9.0 mL deionized water and 27.0 mL ethanol were mixed under stirring at room temperature. Then 0.70 g NaOH and 25.8 mmol fatty acid were added into the above solution and heated to 50 °C to form transparent solution. 0.15 g NaF was dissolved in 18 mL deionized water and then added dropwise to the above solution with vigorous stirring. After aging for 30 min at 50 °C, the mixture was transferred to a 75 mL Teflon-lined autoclave, sealed and heated at 200 °C for 7 h. After the autoclave was cooled to room temperature naturally, the precipitates was collected at the bottom, washed with ethanol and deionized water in sequence, gathered by centrifugation, and then dried in air at 80 °C for 5 h.

Methods of analysis

X-ray powder diffraction patterns (XRD) were measured on a Rigaku D/MAX-2400 with Cu-Kα radiation. The morphologies of the samples were observed by using a Quanta 450 Scanning Electron Microscopy (SEM), a Nova Nanosem 450 field emission scanning electron microscopy (FE-SEM) and a Tecnai G220 S-Twin transmission electron microscopy (TEM).

Results and discussion

Generally, the shape and size of nano/microcrystals synthesized in a solution-based system depend on both the intrinsic structure of the target products and the crystal growth parameters such as the reaction temperature, time, organic ligands, and so forth.[33] In this work, we mainly focus on the effect of the property of organic ligands on the morphologies and growth process of the final β-$NaYF_4$ crystals. The stabilizing ligands we choose include hexanoic acid (HA), caprylic acid (CA), decanoic acid (DA), lauric acid (LA), myristic acid (MA), which all have only one anchoring group and an linear hydrocarbon chain. A series of experiments have been carefully designed with different fatty acid ligands, keeping other controlled parameters fixed, such as the reaction temperature, time, dosage of NaF, NaOH and surfactants.

Morphology. It is obvious that the ligands play a key role in controlling the morphologies of the as-prepared β-$NaYF_4$ samples (Figure 1). Microrods with crown-like ends can form when short chain length ligands are used (HA, Figure 1a). With the increasing of ligand chain length (CA), the microrods shrink to form flower-like microprisms with pointed centers (Figure 1b). A further increase of the ligand chain length (DA, LA and MA) causes the formation of micro/submicrodisks with different aspect ratios (Figure 1c-e). The XRD patterns (Figure S1) confirm that the as-prepared samples are all hexagonal phase (JCPDS card No. 16-0334). Considering the fact that the reaction temperature, reaction time, and reactant concentrations are all the same, the morphology variation should be attributed to the main two factors: pH value and the properties of ligands. In our experiments, the pH values of the reaction system before adding NaF solution were measured (Table 1). Even though the pH values show a regular increase with the chain length, the increase is really slight. So it is rational to ascribe this morphology variation to the difference of ligands. The increase of the melting/boiling point of the fatty acids (Table 1) is strongly dependent on the interligand interaction.[30] Accordingly, the tendency of leaving the crystal surfaces of the ligands decreases with the increase of ligand chain length, so does the surface ligand dynamic population.[30, 31]

Table 1. The pH values of different acid systems; the melting point and boiling point of different acids.

Acid	HA	CA	DA	LA	MA[a]
pH/25 °C	7.12	7.15	7.21	7.24	-
m. p./ °C	-3.9	16	31	40	53
b. p. / °C	205	239	270	299	326

a MA is solid state in the H_2O-EtOH system at 25°C.

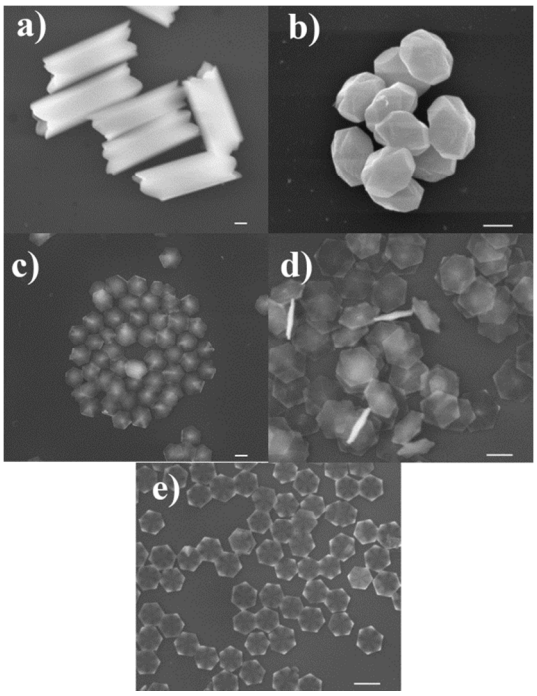

Fig.1 SEM images of β-$NaYF_4$ prepared with different ligands: (a) HA, (b) CA, (c) DA, (d) LA, (e) MA (F/Y=4, n(NaOH)/n(Acid)=0.61, V(H_2O)/V(EtOH)=1.07, 200°C, 7h; the scale bars are all set as 1 μm).

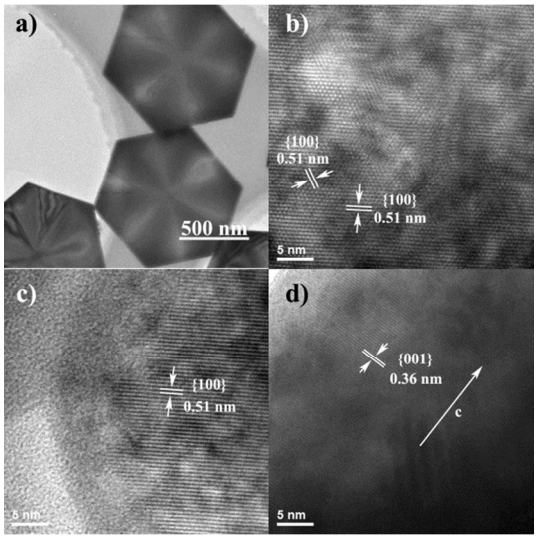

Fig.2 (a) TEM image of β-$NaYF_4$ disks prepared with MA; (b) HRTEM image of the center of a disk; (c) HRTEM image of a corner of a disk; (d) HRTEM image of a β-$NaYF_4$ microrod prepared with HA (F/Y=4,n(NaOH)/n(Acid)=0.61,V(H_2O)/V(EtOH)=1.07, 200°C, 7h).

The tendency of HA ligands leaving the crystal surface is so strong that passivation effect is not obvious, thus the crystals mainly grow along the *c*-axis with a microrod morphology. The high-resolution transmission electron microscopy (HRTEM) image (Figure 2d) clearly shows that the crystal growth is along {001} surfaces.[14, 26, 32] When CA ligands are used, the leaving tendency decreases which makes the crystal dimension shrink along the *c*-axis direction forming microprisms with small aspect ratio. With relative longer hydrocarbon chain length (DA-MA), the leaving tendency decreases significantly which strongly passivates the growth along the *c*-axis but facilitates the growth perpendicular to the sixfold axis, finally resulting in disk-like morphologies with small aspect ratios. Transmission electron microscopy (TEM) image of β-$NaYF_4$ microdisks prepared with MA ligands has been shown in Figure 2a. The {100} lattice fringe estimated from HRTEM images is 0.51 nm (Figure 2b-c), which is in good agreement with the value of 0.515 nm calculated from XRD data (Figure S1, JCPDS card No. 16-0334). A possible growth mechanism of β-$NaYF_4$ in our system is proposed in Figure 3. In addition, β-$NaYF_4$ crystals codoped with 2% Er^{3+} and 20% Yb^{3+} exhibit a similar phenomenon when different fatty acids are used as ligands (Figure 4). When HA is used as ligands, microrods with crown-like ends are formed (Figure 4a). When CA is used, diamond-like microcrystals can be prepared as shown in Figure 4b. When the chain length is increased to 10 (DA), microdisks with sunflower-like top/bottom surfaces can form (Figure 4c). Further increasing the ligand chain length causes the formation of regular hexagonal microcrystals. Moreover, the microdisks prepared with LA ligands possess special spire-like centers (Figure 4e).

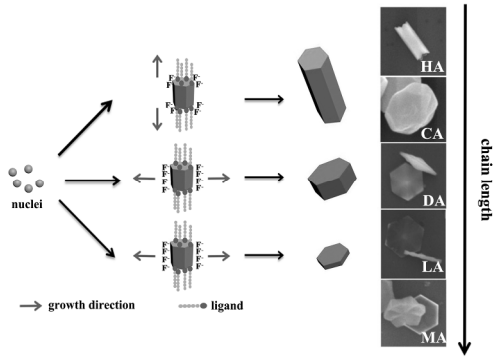

Fig.3 Schematic diagram of the growth process of β-$NaYF_4$ prepared with different ligands.

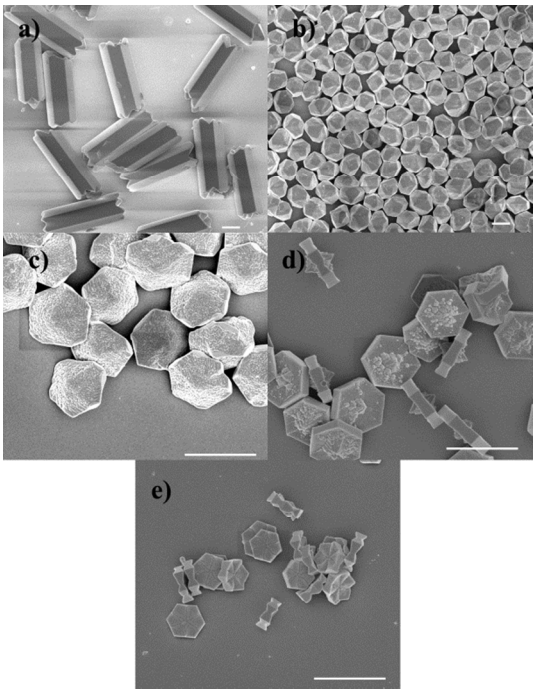

Fig.4 SEM images of β-$NaYF_4$:Yb, Er prepared with different ligands:

(a) HA, (b) CA, (c) DA, (d) LA, (e) MA (F/Re=4, n(NaOH)/n(Acid)=0.61, V(H_2O)/V(EtOH)=1.07, 200°C, 12h; the scale bars are all set as 2 μm).

Growth process. Varying the synthesis conditions, such as the organic ligands, may control over the growth process of β-$NaYF_4$ crystals.[35, 36] In this work, the growth process of β-$NaYF_4$ crystals affected by the ligand dynamics is systematically investigated by quenching the reaction at different time intervals. The SEM results reveal that the growth process of β-$NaYF_4$ crystals is strongly influenced by the ligand dynamics. On the base of the experimental results, the crystal growth process with different ligands from BA to MA can be divided into three groups.

Group I: DA, LA, MA. DA, LA and MA are relatively long chain length ligands with low dynamic property as discussed above. The crystals synthesized with these three kinds of ligands also show a similar growth process. The growth process of $NaYF_4$ crystals prepared with DA ligands by quenching the reaction at different reaction time were investigated by SEM and XRD study as shown in Figure 5. At 2 h, β-$NaYF_4$ hexagonal disks with the diameter about 1.5-1.8 μm are formed at this early stage (Figure 5a) together with some cubic particles according to the XRD results in Figure 5e. When the reaction time was further prolonged to 3 h, 5 h, even to 7h, pure hexagonal $NaYF_4$ are produced (Figure 5e), but the dimensions have not changed remarkably (Figure 5b-d). The growth process of β-$NaYF_4$ with DA ligands can be concluded as a usual dissolution-restructure process: firstly, cubic phase particles are formed; then, α-$NaYF_4$ particles dissolve and β-$NaYF_4$ nanodisks are created nearly simultaneously. β-$NaYF_4$ synthesized with LA and MA ligands experience a similar procedure as well (Figure S2, S3).

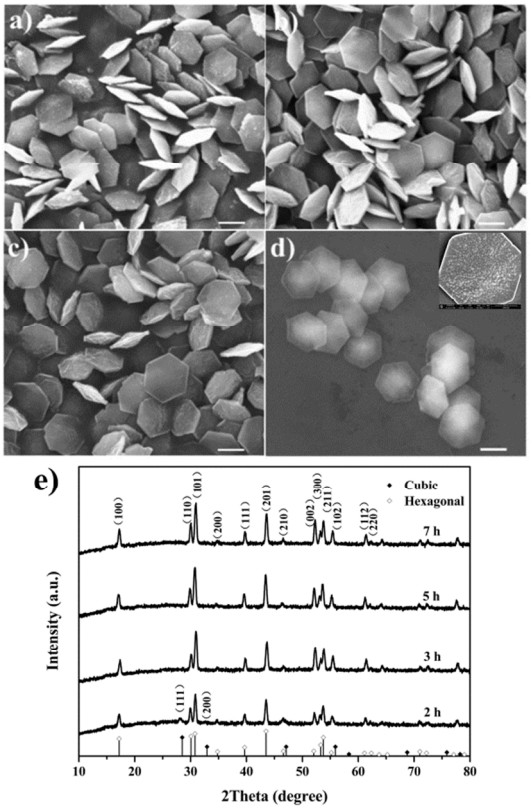

Fig.5 SEM images of β-$NaYF_4$ prepared with DA at different reaction time: (a) 2 h, (b) 3 h, (c) 5 h, (d) 7 h; (e) XRD patterns of $NaYF_4$ (cubic phase: JCPDS card No. 39-0724; hexagonal phase: JCPDS card No. 16-0334) prepared with DA at different reaction time (F/Y=4, n(NaOH)/n(Acid)=0.61, V(H_2O)/V(EtOH)=1.07, 200 °C; the scale bars are all set as 1 μm).

Group II: CA. Unlike fatty acid ligands in Group I, CA is more dynamic than DA, LA and MA. Therefore, the hexagonal crystals with CA as ligands experience a similar but not totally identical growth process. SEM analysis was conducted during the whole experiments at different reaction time as shown in Fig. 4. At 3 h, microprisms with the diameter about 2.0 × 0.6 μm are formed (Figure 6a). With further reaction to 7 h, some microprisms experience a partial dissolution process on the surface of some crystals (Figure 6c). This phenomenon may possibly be caused by the dynamic property of CA ligands, as they possess relatively high tendency of leaving the crystal surfaces, which makes some parts on the surfaces unstable and then dissolve into the reaction media again.

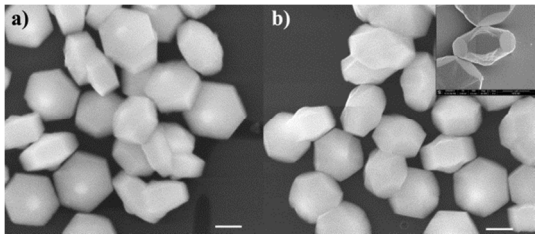

Fig.6 SEM images of β-$NaYF_4$ prepared with CA at different reaction time: (a) 3 h, (c) 7 h (F/Y=4, n(NaOH)/n(Acid)=0.61, V(H_2O)/V(EtOH)=1.07, 200 °C; the scale bars are all set as 1 μm).

Group III: BA, HA. When very short chain length ligands are used, a totally different growth process is discovered by a series of time-dependent SEM studies (Figure 7, S4).

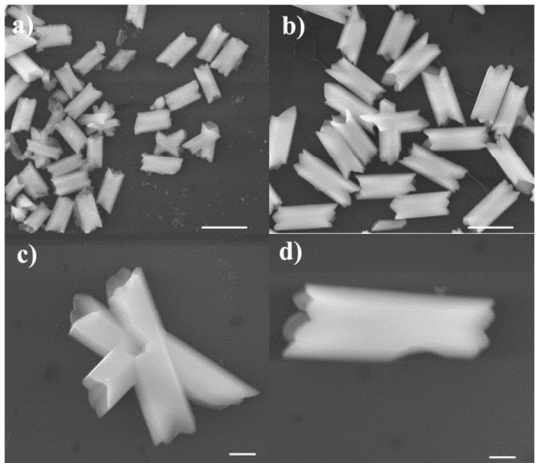

Fig.7 SEM images of β-NaYF4 prepared with HA at different reaction time: (a) 3 h, (b) 5 h, (c, d) 7 h. (F/Y=4, n(NaOH)/n(Acid)=0.61, V(H_2O)/V(EtOH)=1.07, 200 °C; (a, b) the scale bars are all set as 5 μm; (c, d) the scale bars are all set as 2 μm).

For HA system, some flower-like aggregations with the length about 3.5 μm are formed at 3 h (Figure 7a). When the reaction time increases to 5 h and 7 h, the crystals grow into larger dimension about 6.5 μm (length) and the aggregations disappear, leaving small amount of twin or triplet crystals (Figure 7b, c). Careful observation from SEM analysis at 7 h in Fig. 5d, a hollow

defect on the surface of a single microprism appears, which is was the mark of separation of two prisms. In addition, a clear hollow defect in the cross region of a triplet crystal (Figure 7d) proves that a single prism falls from a flower-like aggregation. Short chain length acids such as acetic acid have been widely used to direct the oriented attachment of nanoparticles, owing to their rapid absorbing and leaving on the crystal surface.[31, 37] HA ligands are short with strong tendency to leave the crystal surface, which benefits the aggregation of nuclei. Thus, in HA system, some nuclei should aggregate at early stage, and with the surrounding environment providing reactant, the crystals grow. When the crystals grow to a certain size, extrusion between prisms occurs to form microrods. BA system also experiences a similar growth process (Figure S4). A possible schematic diagram for the growth process is presented in Figure 8.

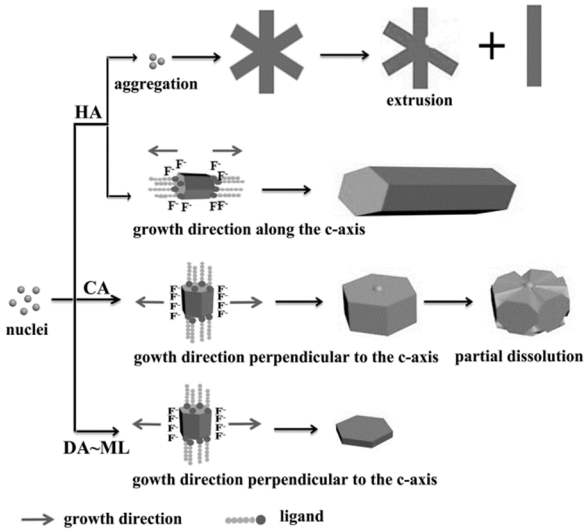

Fig.8 Schematic diagram of the proposed growth processes of the formation of β-$NaYF_4$ with different chain length fatty acids.

Phase transition. It is widely researched and accepted that α→β phase transition of $NaYF_4$ crystals undergoes a dissolution-recrystallization process.[12-14] As we know, α-$NaYF_4$ is metastable and will dissolve under certain conditions, while β-$NaYF_4$ is thermodynamically stable.[35] The α→β phase transition of $NaYF_4$ crystals should be controlled by two main factors: the dissolution of cubic phase and the formation of hexagonal phase. However, based on the above time-dependent experiments (Figure 5, S2, S3), the formation of hexagonal crystals is fast, while the dissolution of α-$NaYF_4$ is slow. Thus, it is rational to regard the entirely dissolving time of α-$NaYF_4$ as the indicator of the rate of α→β phase transition. A series of experiments by quenching the reaction at different intervals with different acids were designed and studied by XRD analysis (Figure 5e, S5). Figure 9 shows the relationship between the dissolving time of α-$NaYF_4$ and the ligand chain length. It is found that there exists a shortest time for the total dissolution ofα-$NaYF_4$ in our system, when CA, DA and LA ligands are used. While when the ligand chain length is longer than LA or shorter than CA, the time needed gets longer. This phenomenon is probably caused by two competitive factors: cubic-phase particle size and ligand dynamic population on crystal surface, which determine the stability of cubic particles. With the chain length increasing, the tendency of ligands leaving the crystal surfaces decreases, and so does the ligand dynamic population. If the ligand dynamic population decreases, the system will be in favor of large nuclei as small ones are not stable. Thus, with large nuclei and high dynamic ligands, the cubic phase crystals will grow into relatively large particles which inhibit the particles dissolve. However, even though long chain ligands from LA to SA can stabilize small nuclei, the weak tendency of leaving the crystal surfaces makes α-$NaYF_4$ particles too stable to redissolve into the reaction media, existing long dissolution time. Owing to the long chain length of SA, the cubic phase still exists when the reaction time is beyond 24 h.

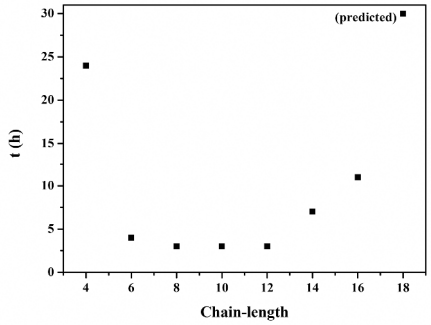

Fig.9 Dependence of the reaction time of total dissolution of α-$NaYF_4$ on the chain length of fatty acid ligands (F/Y=4, n(NaOH)/n(Acid)=0.61，$V(H_2O)/V(EtOH)$=1.07，200 °C).

Conclusions

In summary, the morphology control, crystal growth process and phase transition of β-$NaYF_4$ crystals can be realized utilizing ligand dynamic effect by a hydrothermal method. The ligand dynamics strongly influence the size and shape of β-$NaYF_4$ crystals as the ligand dynamic population varies with different ligand chain length, making the growth direction along or perpendicular to the *c*-axis. In addition, the ligand dynamics affect the growth process of β-$NaYF_4$ crystals by directing the partial dissolution of β-$NaYF_4$ crystals or oriented attachment of the nuclei. Furthermore, the ligand dynamics can control the phase transition of $NaYF_4$ crystals over the dissolution-recrystalization process. The mechanism of how the ligand dynamics influence the morphology, growth process and phase transition is proposed.

Acknowledgement

This work was supported by the National Natural Science Foundation of China (21076038, 21276040).

Notes and references

[a] *E-432 West Campus, No.2 Linggong Road, High-Tech Zone, Dalian, China. Fax: 86 0411 84986264; Tel: 86 0411 84986264; E-mail: wusuli@dlut.edu.cn*

† Electronic Supplementary Information (ESI) available: [The fluorescence spectra and quantum yields (QYs) of CdTe QDs capped with TGA (TGA-CdTe), 4-MBA together with TGA (4-MBA-TGA-CdTe), 4-MBT together with TGA (4-MBT-TGA-CdTe) and 2-MBTH together with TGA (2-MBTH-TGA-CdTe), TEM of CdTe, representations of the electron density distribution for 4-MBA, 4-MBT, 2-MBTH, DPSF and AHMT]. See DOI: 10.1039/b000000x/

1 Y. G. Su, L. P. Li, G. S. Li, *Cryst. Growth Des.*, 2008, **8**, 2678.
2 O. Ehlert, R. Thomann, M. Darbandi, T. Nann, *ACS Nano*, 2008, **2**, 120.
3 E. Downing, L. Hesselink, J. Ralston, R. Macfarlane, *Science*, 1996, **273**, 1185.
4 R. Kumar, M. Nyk, T. Y. Ohulchanskyy, C. A. Flask, P. N. Prasad, *Adv. Funct. Mater.*, 2009, **19**, 853.
5 M. Nyk, R. Kumar, T. Y. Ohulchanskyy, E. J. Bergey, P. N. Prasad, *Nano Lett.*, 2008, **8**, 3834.
6 Z. Wang, C. Liu, L. Chang, Z. Li, *J. Mater. Chem.*, 2012, **22**, 12186.
7 L. Wang, Y. Li, *Chem. Comm.*, 2006, 2557.
8 M. Kumar, P. Zhang, *Biosens. Bioelectron.*, 2010, **25**, 2431.
9 C. J. Carling, J. C. Boyer, N. R. Branda, *J. Am. Chem. Soc.*, 2009, **131**, 10838.
10 C. Yan, A. Dadvand, F. Rosei, D. F. Perepichka, *J. Am. Chem. Soc.*, 2010, **132**, 8868.
11 G. B. Shan, H. Assaaoudi, G. P. Demopoulos, *ACS Appl. Mater. Interfaces*, 2011, **3**, 3239.
12 H. X. Mai, Y. W. Zhang, R. Si, Z. G. Yan, L. D. Sun, L. P. You, C. H. Yan, *J. Am. Chem. Soc.*, 2006, **128**, 6426.
13 R. Komban, J. P. Klare, B. Voss, J. Nordmann, H. J. Steinhoff, M. Haase, *Angew. Chem. Int. Ed.*, 2012, **51**, 6506.
14 F. Zhang, J. Li, J. Shan, L. Xu, D. Zhao, *Chem. Eur. J.*, 2009, **15**, 11010.
15 G. Tian, Z. Gu, L. Zhou, W. Yin, X. Liu, L. Yan, S. Jin, W. Ren, G. Xing, S. Li, Y. Zhao, *Adv. Mater.*, 2012, **24**, 1226.
16 M. Wang, C. C. Mi, W. X. Wang, C. H. Liu, Y. F. Wu, Z. R. Xu, C. B. Mao, S. K. Xu, *ACS Nano*, 2009, **3**, 1580.
17 H. Lee, S. E. Habas, S. Kweskin, D. Butcher, G. A. Somorjai, P. Yang, *Angew. Chem. Int. Ed.*, 2006, **118**, 7988.
18 H. Y. Zhao, Y. F. Wang, J. H. Zeng, *Cryst. Growth Des.*, 2008, 8, 3731.
19 D. Seo, C. I. Yoo, J. C. Park, S. M. Park, S. Ryu, H. Song, *Angew. Chem. Int. Ed.*, 2008, **120**, 775.
20 J. Zhuang, X. Yang, J. Fu, C. Liang, M. Wu,; J. Wang, Q. Su, *Cryst. Growth Des.*, 2013, **13**, 2292.
21 J. Zhuang, J. Wang, X. Yang, I. D. Williams, W. Zhang, Q. Zhang, Z. Feng, Z. Yang, C.Liang, M. Wu, Q. Su, *Chem. Mater.*, 2008, **21**, 160.
22 F. Zhang, Y. Shi, X. Sun, D. Zhao, G. D. Stucky, *Chem. Mater.*, 2009, **21**, 5237.
23 X. Liang, X. Wang, J. Zhuang, Q. Peng, Y. Li, *Inorg. Chem.*, 2007, **46**, 6050.
24 D. Gao, X. Zhang, W. Gao, *ACS Appl. Mater. Interfaces*, 2013, **5**, 9732.
25 J. Zhao, Y. Sun, X. Kong, L. Tian, Y. Wang, L. Tu, J. Zhao, H. Zhang, *J. Phys. Chem. B*, 2008, **112**, 15666.
26 L. Y. Wang, Y. D. Li, *Chem. Mater.*, 2007, **19**, 727.
27 X. Liang, X. Wang, J. Zhuang, Q. Peng, Y. Li, *Inorg. Chem.*, 2007, **46**, 6050.
28 G. S. Yi, G. M. Chow, *Adv. Funct. Mater.*, 2006, **16**, 2324.
29 Y. Yin, A. P. Alivisatos, *Nature*, 2005, **437**, 664.
30 N. Pradhan, D. Reifsnyder, R. Xie, J. Aldana, X. Peng, *J. Am. Chem. Soc.*, 2007, **129**, 9500.
31 B. B. Srivastava, S. Jana, D. D. Sarma, N. Pradhan, *J. Phys. Chem. Lett.*, 2010, **1**, 1932.
32 F. Zhang, Y. Wan, T. Yu, F. Zhang, Y. Shi, S. Xie, Y. Li, L. Xu, B. Tu, D. Zhao, *Angew. Chem. Int. Ed.*, 2007, **46**, 7976.
33 C. Li, C. Zhang, Z. Hou, L. Wang, Z. Quan, H. Lian, J. Lin, *J. Phys. Chem. C*, 2009, **113**, 2332.
34 Y. Jun, J. Choi, J. Cheon, *Angew. Chem. Int. Ed.*, 2006, **45**, 3414.`
35 X. Liang, X. Wang, J. Zhuang, Q. Peng, Y. Li, *Adv. Funct. Mater.*, 2007, **17**, 2757.
36 F. Tao, F. Pan, Z. Wang, W. Cai, L.Yao, *CrystEngComm.*, 2010, **12**, 4263.
37 A. J. Houtepen, R. Koole, D. Vanmaekelbergh, J. Meeldijk, S. G. Hickey, *J. Am. Chem. Soc.*, 2006, **128**, 6792.